Supplementary Information

Figure S1: Location of recordings within the inferior colliculus pg 2

Figure S2: Consonant identification with different classifiers and neural representations pg 4

Figure S3: Consonant identification with different population sizes pg 6

Figure S4: Identifying single units based on persistence pg 7

Figure S5: Noise correlations in IC populations are negligible pg 9

Table S1: Details of statistical analyses pg 10

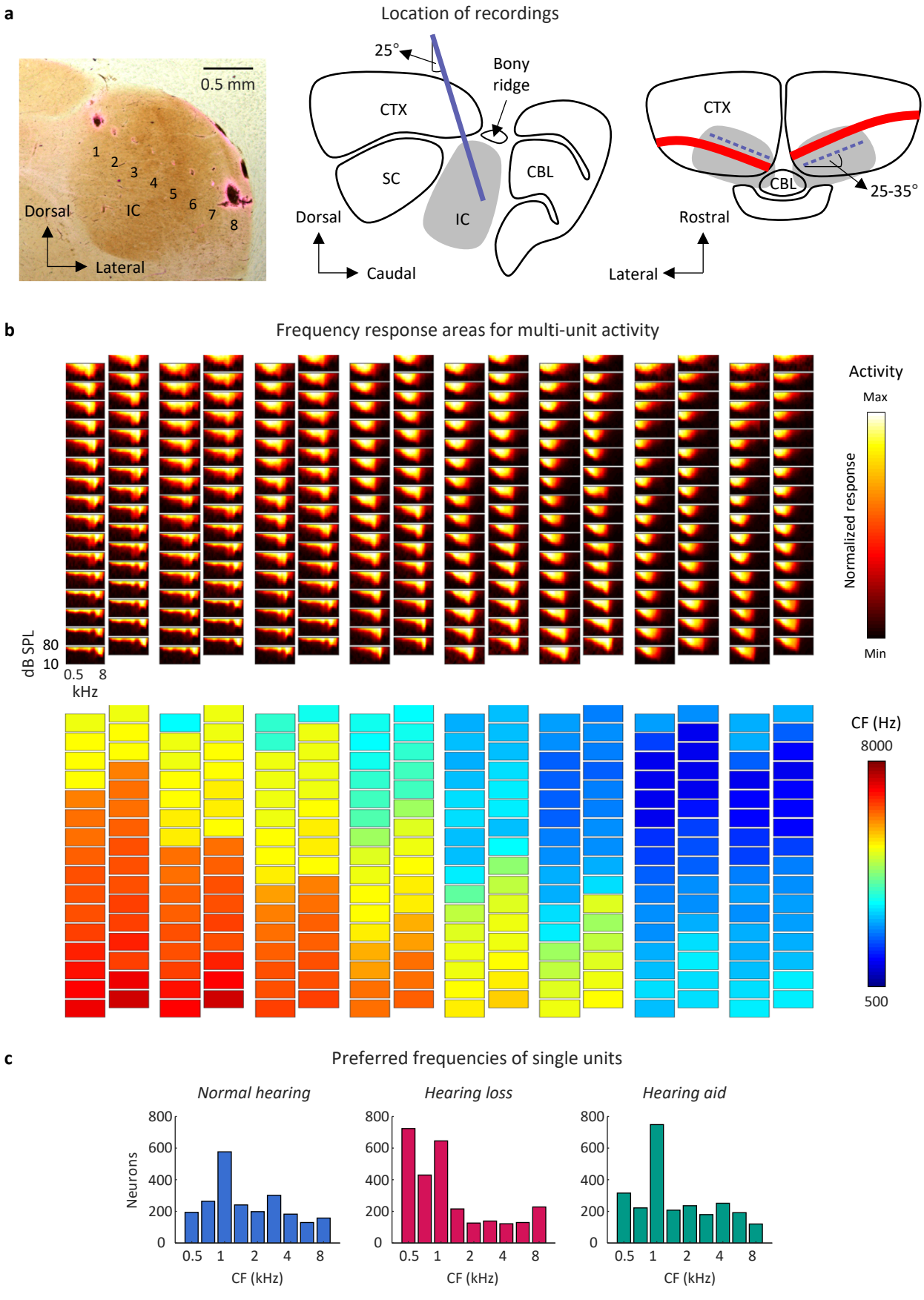

Figure S1: Location of recordings within the inferior colliculus *(continued…)*

Figure S1: Location of recordings within the inferior colliculus

The geometry of our electrode arrays was designed specifically to match the layout of the speech-sensitive area in the central nucleus of the gerbil IC. The recording sites spanned a plane measuring 1.4 mm x 0.45 mm. When oriented approximately parallel to the coronal plane, one array covered the entire mediolateral extent of the central nucleus in one hemisphere and enough of its dorsoventral extent to sample from the relevant frequency layers (preferred frequencies up to ~10 kHz). (a) The left panel shows a merge of brightfield and fluorescent images of a coronal section taken for cytochrome oxidase and DiI staining, respectively (the electrode array was coated with DiI and, thus, the fluorescent areas indicate the position of each of the 8 shanks of the array within the section). This image is an example from a single animal. We did not routinely confirm the location of our recordings through histology but instead relied on the physiological properties of the MUA as illustrated in b. The approach to the IC was constrained by the locations of a large blood vessel on the surface of the brain and a bony ridge that protrudes from the lateral wall of the skull between the cortex and midbrain, both of which varied from animal to animal and across hemispheres in the same animal. The electrode arrays were rotated by a fixed angle of 25° relative to the coronal plane about the mediolateral axis to avoid the bony ridge (see middle panel with array (blue), IC (gray), and surrounding structures) and a variable angle of 25-35° relative to the coronal plane about the dorsoventral axis to align with the blood vessel (see right panel with array shanks (blue), blood vessels (red), IC (gray), and surrounding structures). The position of the electrode arrays along the mediolateral axis was fixed but the position along the rostrocaudal axis was varied from animal to animal and across hemispheres in the same animal to avoid the blood vessel. Thus, across animals and hemispheres, the recordings sampled the full three-dimensional volume of the central nucleus. (b) MUA recorded in the inferior colliculus during the presentation of tones. The top panel shows the MUA FRAs for all 256 channels on one electrode array from an example normal hearing animal. The colormap for each plot is normalized to the minimum and maximum activity level across all frequencies and intensities. The bottom panel indicates the center frequency (the frequency for which the mean MUA was more than 3 standard deviations above the mean MUA during silence at the lowest intensity) for each channel. (c) The distribution of center frequencies (CFs) of single units in our sample for which responses to tones were recorded for animals with normal hearing (left; n = 2249) and animals with hearing loss without (middle; n = 2959) and with (right; n = 2664) a hearing aid. The CF was defined as the frequency at which the response to a tone was significantly greater than responses recorded during silence at the lowest intensity (probability of observed spike count $p < 0.01$ assuming Poisson-distributed counts; no correction was made for multiple comparisons). The overrepresentation of 1 kHz is consistent with the oversized “pars lateralis” of the IC in the gerbil (Cant, Front. Neural Circuits, 2013). The distribution of CFs shifted toward lower frequencies with hearing loss, consistent with the observed effects of noise-induced hearing loss on peripheral tuning (Henry et al., J. Neurosci, 2016), but was similar to normal with the hearing aid.

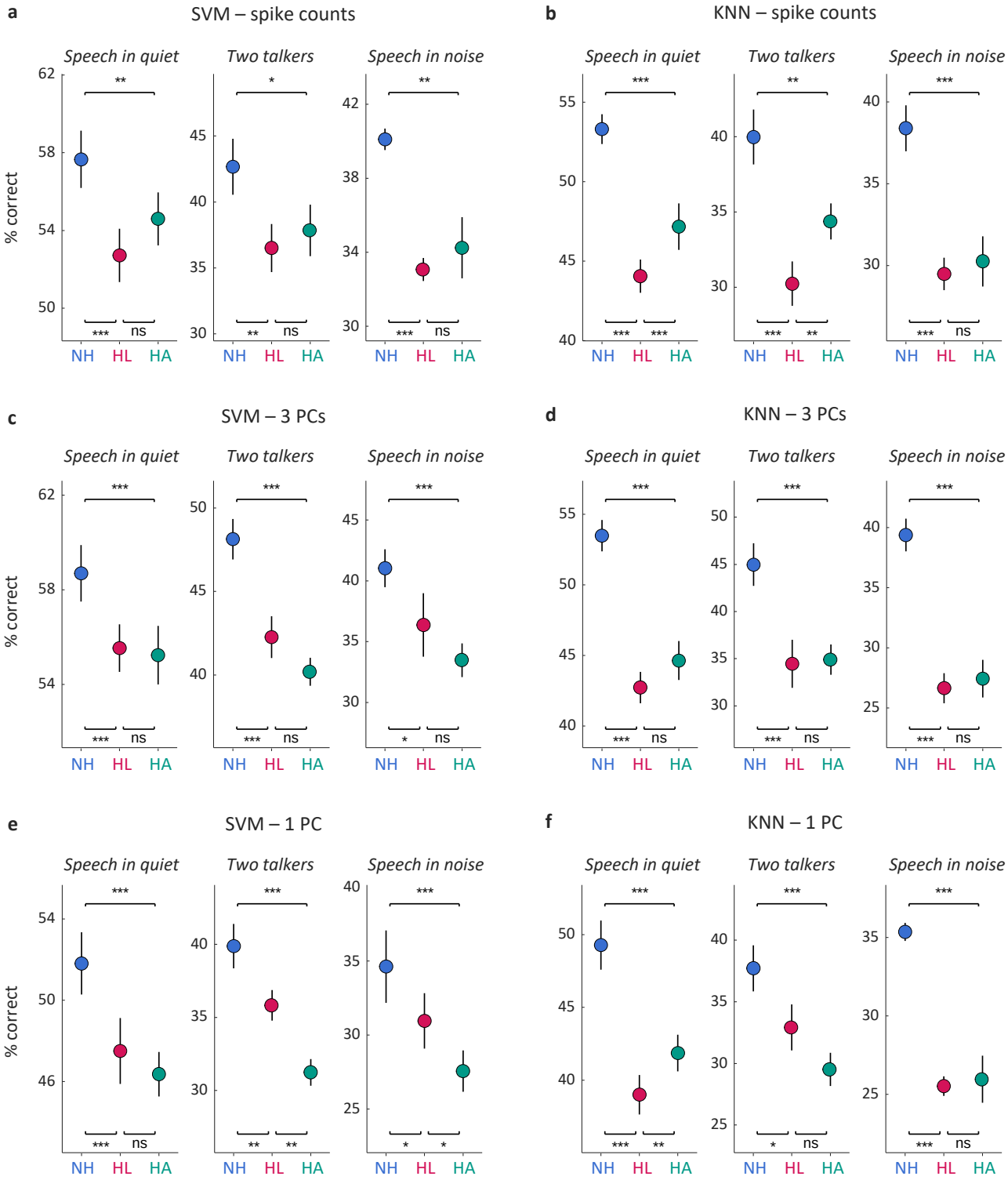

Figure S2: Consonant identification with different classifiers and neural representations *(continued…)*

Figure S2: Consonant identification with different classifiers and neural representations

The figure shows the performance of different classifiers trained to identify consonants based on population responses to speech at 62 dB SPL with different response representations. In all cases, the first 150 ms of single-trial responses of populations of 150 neurons were used. Populations were formed by sampling at random, without replacement, from neurons from all animals until there were no longer enough neurons remaining to form another population. For each classifier and neural representation, results are shown (mean ± 95% confidence intervals derived from bootstrap resampling across populations) for three conditions: speech in quiet, speech in the presence of ongoing speech from a second talker at equal intensity, and speech in the presence of multi-talker babble noise at equal intensity. (a) Performance of a support vector machine trained to classify the total spike counts. The details of the support vector machine were identical to those used in the Results. (b) Performance of a k-nearest neighbors classifier trained to classify the total spike counts with 10-fold cross validation. The values shown are for k = 16 which had the highest cross-validated performance. (c) Performance of a support vector machine trained to classify the responses after projection onto the three principal components that best described the variance in responses across the entire population (reducing the response of the entire population to three values in each 5 ms time bin as in Figure 2b). (d) Performance of a k-nearest neighbors classifier trained to classify the responses after projection onto the first three principal components. (e) Performance of a support vector machine trained to classify the responses after projection onto the principal component that best described the variance in responses across the entire population (reducing the response of the entire population to one value in each 5 ms time bin). (f) Performance of a k-nearest neighbors classifier trained to classify the responses after projection onto the first principal component.

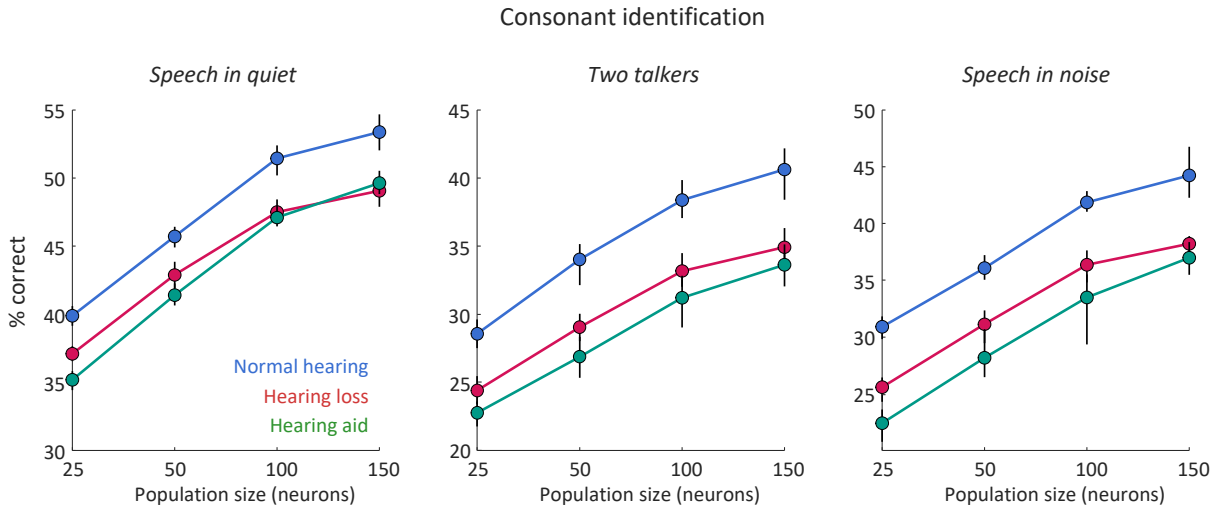

Figure S3: Consonant identification with different population sizes

The figure shows the performance of a support vector machine trained to identify consonants based on population responses to speech at 62 dB SPL. Populations were formed by sampling at random, without replacement, from neurons from all animals until there were no longer enough neurons remaining to form another population. Responses were the first 150 ms of single-trial responses represented as spike counts with 5 ms time bins. Results are shown for different populations sizes (mean ± 95% confidence intervals derived from bootstrap resampling across populations) for three conditions: speech in quiet, speech in the presence of ongoing speech from a second talker at equal intensity, and speech in the presence of multi-talker babble noise at equal intensity. The number of independent populations for each population size and each condition were as follows for speech in quiet: population size of 25 neurons, NH (n = 90), HL (n = 126), HA (n = 120); population size of 50 neurons, NH (n = 45), HL (n = 63), HA (n = 60); population size of 100 neurons, NH (n = 23), HL (n = 32), HA (n = 30); population size of 150 neurons, NH (n = 15), HL (n = 21), HA (n = 20). The number of independent populations for each population size and each condition were as follows for two talkers: population size of 25 neurons, NH (n = 36), HL (n = 60), HA (n = 36); population size of 50 neurons, NH (n = 18), HL (n = 30), HA (n = 18); population size of 100 neurons, NH (n = 9), HL (n = 15), HA (n = 9); population size of 150 neurons, NH (n = 6), HL (n = 10), HA (n = 6). The number of independent populations for each population size and each condition were as follows for speech in noise: population size of 25 neurons, NH (n = 30), HL (n = 54), HA (n = 36); population size of 50 neurons, NH (n = 15), HL (n = 27), HA (n = 18); population size of 100 neurons, NH (n = 8), HL (n = 14), HA (n = 9); population size of 150 neurons, NH (n = 5), HL (n = 9), HA (n = 6).

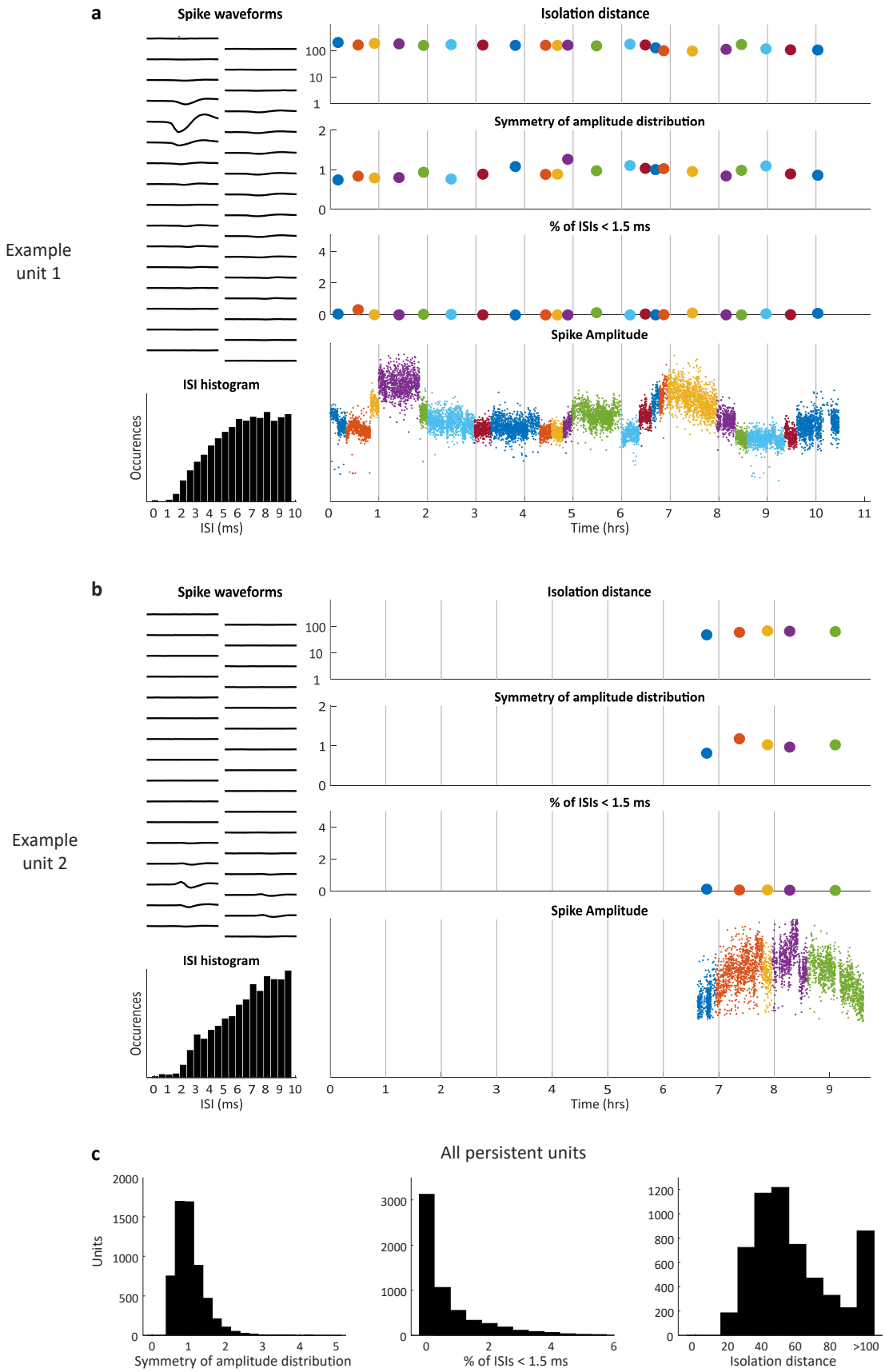

Figure S4: Identifying single units based on persistence *(continued…)*

Figure S4: Identifying single units based on persistence

(a) An example unit that was present during an entire 10-hour recording session. The left column shows the average waveform for the unit on each of 32 electrode channels as well as the histogram of its interspike intervals. The right column shows the values of several quantities for the unit at different time points in the recording, with colors corresponding to different overlapping segments of the response as described in the Methods: (1) Isolation distance (Schmitzer-Torbert et al., 2005), which is calculated by assuming that each cluster forms a multi-dimensional Gaussian cloud in feature space and measures, in terms of the standard deviation of the original cluster, the increase in the size of the cluster required to double the number of snippets within it. A large isolation distance indicates that the cluster is well separated from other clusters, with a value of 20 typically used as a threshold for classifying a cluster as a single unit. (2) The symmetry of the spike amplitude distribution, which is measured as $(a_{16} - a_{2.5})/(a_{97.5} - a_{84})$, where a_x is the spike amplitude corresponding the x^{th} percentile of the distribution of all amplitudes for that unit. A value significantly less than 1 indicates that the amplitude distribution has been truncated, i.e. that the threshold for spike detection is not low enough to capture all spikes from the unit. (3) The percentage of interspike intervals that are less than 1.5 ms, the typical absolute refractory period for IC neurons. A large value indicates that the cluster contains spikes from more than 1 unit. (4) The RMS amplitude of every spike waveform. (b) A second example unit that was only identified during the latter stages of a recording. (c) Histograms of amplitude symmetry, percentage of interspike intervals < 1.5 ms, and isolation distance for all clusters that were continuously present in a recording for at least 2.5 hours.

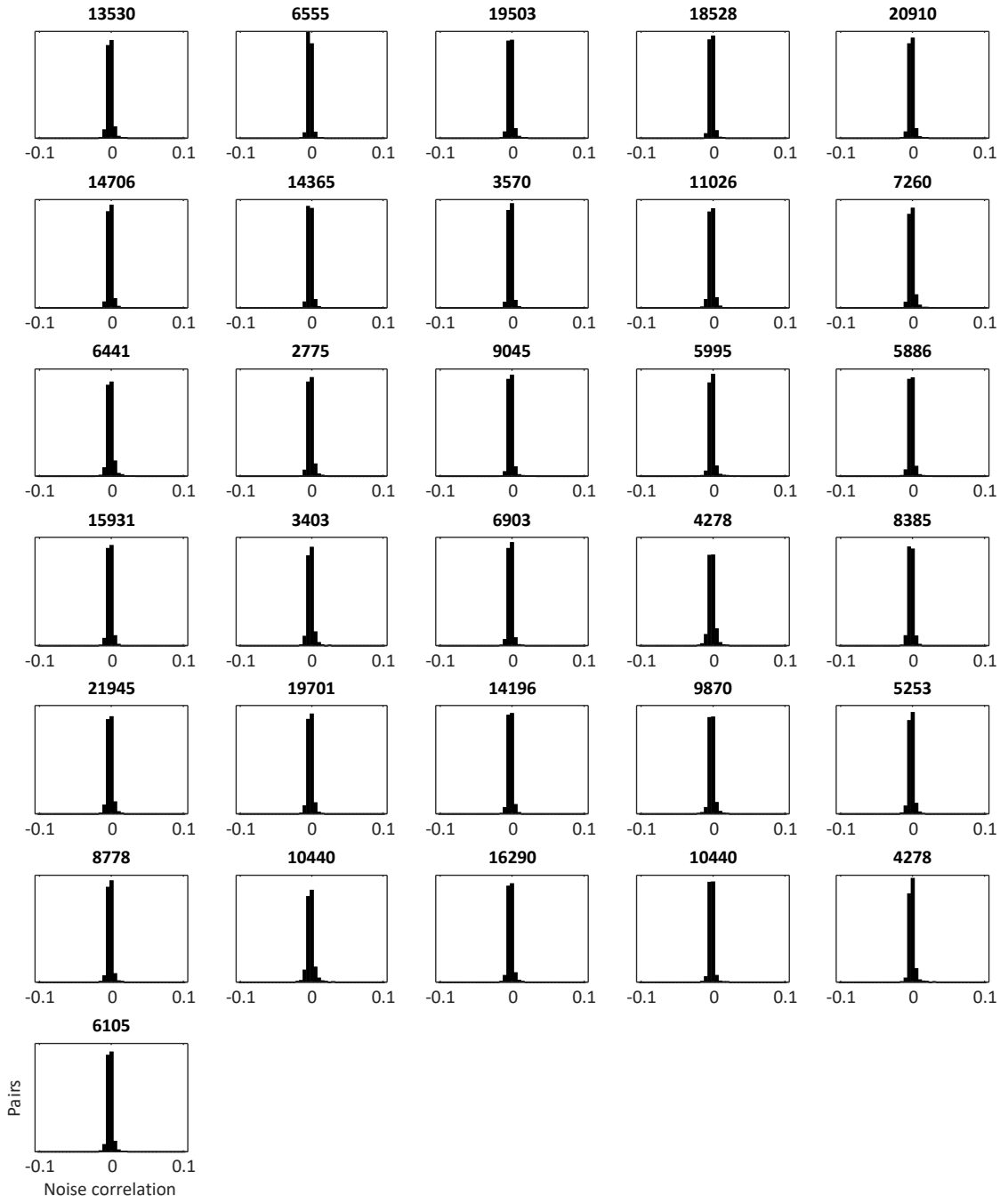

Figure S5: Noise correlations in IC populations are negligible

Each panel shows the distribution of noise correlations in the responses to repeated trials of identical speech at 62 dB SPL of simultaneously recorded pairs of neurons from one animal. To compute correlations, responses to all syllables were concatenated in time and converted to binary spike count vectors with 1 ms time bins. For each neuron on each trial, the noise was measured as the difference between the response on that single trial and the mean response across trials. The total number of pairs for each experiment is indicated above each panel. Only the 31 of 35 animals for which two trials of identical speech were presented are shown.

TABLE S1: Details of statistical analyses

This table provides the details of the statistical tests used in this study, including test type, sampling unit, sample sizes, and p-values. For all analyses of single neuron response properties for which distributions were not necessarily normal, non-parametric tests were used. For all analyses of classifier performance with population responses, parametric tests were used. In cases where comparisons were made across more than two groups, post hoc tests were used to compute pairwise p-values.

FIGURE 3		
3B	Kruskal–Wallis with post-hoc Tukey-Kramer	
	Sampling unit: single neurons	
	Groups: NH (n = 2302), HL (n = 3186), HA (n = 3066)	
	NH vs. HL	p < 1e-9
	NH vs. HA	p = 0.724
	HL vs. HA	p < 1e-9
3C	One-way ANOVA with post-hoc Tukey-Kramer	
	Sampling unit: single neurons	
	Groups: NH (n = 2302), HL (n = 3186), HA (n = 3066)	
	NH vs. HL	p < 1e-9
	NH vs. HA	p = 0.904
	HL vs. HA	p < 1e-9
3D, left	One-way ANOVA with post-hoc Tukey-Kramer	
	Sampling unit: populations of 150 neurons	
	Groups: NH (n = 15), HL (n = 21), HA (n = 20)	
	NH vs. HL	p = 4.619635e-05
	NH vs. HA	p = 4.295917e-04
	HL vs. HA	p = 0.780
3D, center	One-way ANOVA with post-hoc Tukey-Kramer	
	Sampling unit: populations of 150 neurons	
	Groups: NH (n = 6), HL (n = 10), HA (n = 6)	
	NH vs. HL	p = 1.608439e-04
	NH vs. HA	p = 6.829283e-05
	HL vs. HA	p = 0.558
3D, right	One-way ANOVA with post-hoc Tukey-Kramer	
	Sampling unit: populations of 150 neurons	
	Groups: NH (n = 5), HL (n = 9), HA (n = 6)	
	NH vs. HL	p = 0.002
	NH vs. HA	p = 5.860694e-04
	HL vs. HA	p = 0.591

FIGURE 4		
4C, left	Kruskal–Wallis with post-hoc Tukey-Kramer	
	Sampling unit: single neurons	
	Groups: NH (n = 2111), HL (n = 2228), HA (n = 2111)	
	NH vs. HL	p < 1e-9
	NH vs. HA	p = 0.666
	HL vs. HA	p < 1e-9
4C, middle left	Kruskal–Wallis with post-hoc Tukey-Kramer	
	Sampling unit: single neurons	
	Groups: NH (n = 2111), HL (n = 2228), HA (n = 2111)	
	NH vs. HL	p < 1e-9
	NH vs. HA	p = 0.017
	HL vs. HA	p < 1e-9
4C, middle right	Kruskal–Wallis with post-hoc Tukey-Kramer	
	Sampling unit: single neurons	
	Groups: NH (n = 2111), HL (n = 2228), HA (n = 2111)	
	NH vs. HL	p < 1e-9
	NH vs. HA	p = 0.659
	HL vs. HA	p < 1e-9

4C, right

Kruskal–Wallis with post-hoc Tukey-Kramer

Sampling unit: single neurons

Groups: NH (n = 2111), HL (n = 2228), HA (n = 2111)

NH vs. HL	p < 1e-9
NH vs. HA	p < 1e-9
HL vs. HA	p = 0.121

4E

Kruskal–Wallis with post-hoc Tukey-Kramer

Sampling unit: single neurons

Groups: NH (n = 2111), HL (n = 2228), HA (n = 2111)

NH vs. HL	p < 1e-9
NH vs. HA	p = 3.411576e-09
HL vs. HA	p = 0.364

FIGURE 5

5C

One-way ANOVA with post-hoc Tukey-Kramer

Sampling unit: single neurons

Groups: NH (n = 2249), HL (n = 2959), HA (n = 2664)

NH vs. HL	p = 2.363455e-04
NH vs. HA	p = 0.068
HL vs. HA	p = 1.177518e-09

5D

One-way ANOVA with post-hoc Tukey-Kramer

Sampling unit: single neurons

Groups: NH (n = 2249), HL (n = 2959), HA (n = 2664)

NH vs. HL	p = 0.007
NH vs. HA	p = 0.978
HL vs. HA	p = 0.003

5E

One-way ANOVA with post-hoc Tukey-Kramer

Sampling unit: single neurons

Groups: NH (n = 2249), HL (n = 2959), HA (n = 2664)

NH vs. HL	p < 1e-9
NH vs. HA	p = 0.037
HL vs. HA	p < 1e-9

5F

Kruskal–Wallis with post-hoc Tukey-Kramer

Sampling unit: single neurons

Groups: NH (n = 2249), HL (n = 2959), HA (n = 2664)

NH vs. HL	p = 0.470
NH vs. HA	p = 0.021
HL vs. HA	p = 1.289725e-04

5G

One-way ANOVA with post-hoc Tukey-Kramer

Sampling unit: populations of 10 neurons

Groups: NH (n = 224), HL (n = 295), HA (n = 266)

NH vs. HL	p = 1.142218e-09
NH vs. HA	p = 0.921
HL vs. HA	p = 1.320555e-09

FIGURE 6

6C

Paired t-test, two-sided

Sampling unit: single cross-validation fold

Groups: Original (n = 10), after HA (n = 10)

p = 0.002

6D

One-way ANOVA with post-hoc Tukey-Kramer

Sampling unit: populations of 150 neurons

Groups: NH (n = 15), HL (n = 21), HA (n = 20), HL+20dB (n = 21)

NH vs. HL	p = 3.549274e-05
NH vs. HA	p = 4.310342e-04
NH vs. HL+20dB	p = 0.855
HL vs. HA	p = 0.900

	HL vs. HL+20dB	p = 1.626763e-04
	HA vs. HL+20dB	p = 0.002
6E	Kruskal–Wallis with post-hoc Tukey-Kramer	
	Sampling unit: single neurons	
	Groups: NH (n = 2302), HL (n = 3186), HA (n = 3066), HL+20dB (n = 3153)	
	NH vs. HL	p = 3.782072e-09
	NH vs. HA	p = 8.734549e-06
	NH vs. HL+20dB	p = 0.236
	HL vs. HA	p = 0.093
	HL vs. HL+20dB	p = 3.768258e-09
	HA vs. HL+20dB	p = 3.770109e-09
6F, left	One-way ANOVA with post-hoc Tukey-Kramer	
	Sampling unit: populations of 150 neurons	
	Groups: NH (n = 5), HL (n = 9), HA (n = 6), HL+20dB (n = 9)	
	NH vs. HL	p = 0.001
	NH vs. HA	p = 2.755971e-04
	NH vs. HL+20dB	p = 0.443
	HL vs. HA	p = 0.731
	HL vs. HL+20dB	p = 0.014
	HA vs. HL+20dB	p = 0.003
6F, right	One-way ANOVA with post-hoc Tukey-Kramer	
	Sampling unit: populations of 150 neurons	
	Groups: NH (n = 6), HL (n = 10), HA (n = 6), HL+20dB (n = 9)	
	NH vs. HL	p = 5.603490e-05
	NH vs. HA	p = 1.885043e-05
	NH vs. HL+20dB	p = 0.003
	HL vs. HA	p = 0.692
	HL vs. HL+20dB	p = 0.380
	HA vs. HL+20dB	p = 0.083

FIGURE 7

7A, left	Unpaired t-test, two-sided
	Sampling unit: populations of 150 neurons
	Groups: NH (n = 15), NH+20dB (n = 15)
	p = 0.374
7A, middle	Unpaired t-test, two-sided
	Sampling unit: populations of 150 neurons
	Groups: NH (n = 5), NH+20dB (n = 5)
	p = 0.233
7A, right	Unpaired t-test, two-sided
	Sampling unit: populations of 150 neurons
	Groups: NH (n = 6), NH+20dB (n = 6)
	p = 0.045
7B, left	Wilcoxon rank sum, two-sided
	Sampling unit: single neurons
	Groups: NH (n = 1035), NH+20dB (n = 1035)
	NH vs. HL p = 0.217
7B, middle	Wilcoxon rank sum, two-sided
	Sampling unit: single neurons
	Groups: NH (n = 1035), NH+20dB (n = 1035)
	NH vs. HL p = 0.574
7B, right	Wilcoxon rank sum, two-sided
	Sampling unit: single neurons
	Groups: NH (n = 1035), NH+20dB (n = 1035)
	NH vs. HL p = 0.001

7C

Unpaired t-test, two-sided

Sampling unit: populations of 150 neurons

Groups: NH (n = 6), NH+20dB (n = 9)

NH vs. NH+20dB p = 0.903

FIGURE S2

row 1, column 1

One-way ANOVA with post-hoc Tukey-Kramer

Sampling unit: populations of 150 neurons

Groups: NH (n = 15), HL (n = 21), HA (n = 20)

NH vs. HL p = 1.196366e-05
NH vs. HA p = 0.007
HL vs. HA p = 0.096

row 1, column 2

One-way ANOVA with post-hoc Tukey-Kramer

Sampling unit: populations of 150 neurons

Groups: NH (n = 6), HL (n = 10), HA (n = 6)

NH vs. HL p = 0.001
NH vs. HA p = 0.020
HL vs. HA p = 0.633

row 1, column 3

One-way ANOVA with post-hoc Tukey-Kramer

Sampling unit: populations of 150 neurons

Groups: NH (n = 5), HL (n = 9), HA (n = 6)

NH vs. HL p = 1.292813e-04
NH vs. HA p = 0.002
HL vs. HA p = 0.613

row 1, column 4

One-way ANOVA with post-hoc Tukey-Kramer

Sampling unit: populations of 150 neurons

Groups: NH (n = 15), HL (n = 21), HA (n = 20)

NH vs. HL p < 1e-9
NH vs. HA p = 9.467359e-09
HL vs. HA p = 6.716346e-04

row 1, column 5

One-way ANOVA with post-hoc Tukey-Kramer

Sampling unit: populations of 150 neurons

Groups: NH (n = 6), HL (n = 10), HA (n = 6)

NH vs. HL p = 4.082242e-07
NH vs. HA p = 0.001
HL vs. HA p = 0.007

row 1, column 6

One-way ANOVA with post-hoc Tukey-Kramer

Sampling unit: populations of 150 neurons

Groups: NH (n = 5), HL (n = 9), HA (n = 6)

NH vs. HL p = 1.929791e-06
NH vs. HA p = 1.750706e-05
HL vs. HA p = 0.768

row 2, column 1

One-way ANOVA with post-hoc Tukey-Kramer

Sampling unit: populations of 150 neurons

Groups: NH (n = 15), HL (n = 21), HA (n = 20)

NH vs. HL p = 2.286552e-04
NH vs. HA p = 6.980138e-05
HL vs. HA p = 0.902

row 2, column 2

One-way ANOVA with post-hoc Tukey-Kramer

Sampling unit: populations of 150 neurons

Groups: NH (n = 6), HL (n = 10), HA (n = 6)

NH vs. HL p = 3.395562e-05
NH vs. HA p = 2.690555e-06
HL vs. HA p = 0.122

row 2, column 3 One-way ANOVA with post-hoc Tukey-Kramer

Sampling unit: populations of 150 neurons

Groups: NH (n = 5), HL (n = 9), HA (n = 6)

NH vs. HL	p = 0.021
NH vs. HA	p = 9.447568e-04
HL vs. HA	p = 0.151

row 2, column 4 One-way ANOVA with post-hoc Tukey-Kramer

Sampling unit: populations of 150 neurons

Groups: NH (n = 15), HL (n = 21), HA (n = 20)

NH vs. HL	p < 1e-9
NH vs. HA	p = 1.012149e-09
HL vs. HA	p = 0.124

row 2, column 5 One-way ANOVA with post-hoc Tukey-Kramer

Sampling unit: populations of 150 neurons

Groups: NH (n = 6), HL (n = 10), HA (n = 6)

NH vs. HL	p = 8.630276e-05
NH vs. HA	p = 4.820975e-04
HL vs. HA	p = 0.972

row 2, column 6 One-way ANOVA with post-hoc Tukey-Kramer

Sampling unit: populations of 150 neurons

Groups: NH (n = 5), HL (n = 9), HA (n = 6)

NH vs. HL	p = 1.364779e-07
NH vs. HA	p = 1.033488e-06
HL vs. HA	p = 0.821

row 3, column 1 One-way ANOVA with post-hoc Tukey-Kramer

Sampling unit: populations of 150 neurons

Groups: NH (n = 15), HL (n = 21), HA (n = 20)

NH vs. HL	p = 2.379558e-05
NH vs. HA	p = 2.672355e-07
HL vs. HA	p = 0.338

row 3, column 2 One-way ANOVA with post-hoc Tukey-Kramer

Sampling unit: populations of 150 neurons

Groups: NH (n = 6), HL (n = 10), HA (n = 6)

NH vs. HL	p = 0.006
NH vs. HA	p = 5.547881e-06
HL vs. HA	p = 0.002

row 3, column 3 One-way ANOVA with post-hoc Tukey-Kramer

Sampling unit: populations of 150 neurons

Groups: NH (n = 5), HL (n = 9), HA (n = 6)

NH vs. HL	p = 0.038
NH vs. HA	p = 4.693988e-04
HL vs. HA	p = 0.043

row 3, column 4 One-way ANOVA with post-hoc Tukey-Kramer

Sampling unit: populations of 150 neurons

Groups: NH (n = 15), HL (n = 21), HA (n = 20)

NH vs. HL	p < 1e-9
NH vs. HA	p = 2.249799e-09
HL vs. HA	p = 0.006

row 3, column 5 One-way ANOVA with post-hoc Tukey-Kramer

Sampling unit: populations of 150 neurons

Groups: NH (n = 6), HL (n = 10), HA (n = 6)

NH vs. HL	p = 0.015
NH vs. HA	p = 3.720145e-04
HL vs. HA	p = 0.094

row 3, column 6 One-way ANOVA with post-hoc Tukey-Kramer

Sampling unit: populations of 150 neurons

Groups: NH (n = 5), HL (n = 9), HA (n = 6)

NH vs. HL	p = 9.302858e-07
NH vs. HA	p = 5.030270e-06
HL vs. HA	p = 0.925